Journal of Alloys and Compounds 509 (2011) 7723–7728

Contents lists available at ScienceDirect

Journal of Alloys and Compounds

journal homepage: www.elsevier.com/locate/jallcom

Controlled crystallite orientation in ZnO nanorods prepared by chemical bath deposition: Effect of H_2O_2

K.V. Gurav[a], U.M. Patil[a], S.M. Pawar[b], J.H. Kim[b], C.D. Lokhande[a,*]

[a] Thin Film Physics Laboratory, Department of Physics, Shivaji University, Kolhapur 416004 (M. S.), India
[b] Photonic and Electronic Thin Film Laboratory, Department of Materials Science and Engineering, Chonnam National University, Gwangju 500-757, South Korea

ARTICLE INFO

Article history:
Received 14 January 2011
Received in revised form 13 April 2011
Accepted 16 April 2011
Available online 23 April 2011

Keywords:
Chemical method
ZnO nanorods
X-ray diffraction
SEM
Optical studies

ABSTRACT

ZnO nanorods with controlled crystallite orientation are grown on glass substrate by chemical bath deposition (CBD) method via hydrogen peroxide (H_2O_2) route. The crystallite orientation in the film is successfully controlled by varying content of H_2O_2 in the bath solution. The crystallites became increasingly oriented as content of H_2O_2 in the bath solution increased, resulting in the formation of vertically aligned ZnO nanorods. The possible growth mechanism for the vertically aligned ZnO nanorods is proposed. The influence of content of H_2O_2 in the bath solution on structural, surface morphological, electrical and optical properties is studied and reported.

1. Introduction

Zinc oxide (ZnO) possesses variety of nanostructures and it is the next most important material after carbon nanotubes [1]. Out of various nanoforms of ZnO, nanorod is such a morphology that has received a great deal of attention in recent years, because of its unique optoelectronic, mechanical, magnetic and chemical properties which provide various potential applications. Recently, the report on room temperature lasing action of highly oriented nanorod array of ZnO has demonstrated that the functional design of ZnO nanomaterials in a highly oriented and ordered array is crucial for the development of the novel devices [2]. Various chemical and physical deposition techniques have reportedly created an oriented structure of ZnO nanorods with average diameters typically ranging over an order of magnitude from 20 to 200 nm. For instance, catalytic growth via the liquid–solid–vapor epitaxy (VLSE) mechanism [3], metal-organic chemical vapor deposition (MOCVD) [4], pulsed laser deposition (PLD) [5] and epitaxial electrodeposition [6] have been particularly successful in creating highly oriented arrays of nanorods of ZnO. Out of these, CBD is a soft chemical method to deposit ZnO nanorods. However the coating of a substrate with nanosized ZnO seeds [7] or making use of templates [8] are the prerequisite conditions for the growth of vertically aligned ZnO nanorods. Thus, it is still a challenge to fabricate vertically aligned ZnO nanorods arrays to a sub-100 nm regime at a low temperature, seedless and template free deposition method.

In the present work, we are particularly successful in creating vertically aligned ZnO nanorod arrays. The strategy to design nanostructured thin film is entirely based on a wet chemical, bottom up approach; such an approach does not require any template, membrane, surfactant or applied external field to create nanoparticles or to control their orientation. The vertically aligned arrays of ZnO nanorods are grown onto glass substrate by CBD method via hydrogen peroxide (H_2O_2) route. The different preparative parameters, such as bath temperature, concentration of precursor solution, pH of the bath and quantity of H_2O_2 in the bath solution are optimized to get vertically aligned ZnO nanorods. However, The as-deposited film consists of mixture of zinc hydroxide [$Zn(OH)_2$] and ZnO [9–11]. Therefore, in the present work, to get phase pure ZnO film, the as-deposited ZnO films are annealed in air at 673 K for 2 h. The quantity of H_2O_2 added in the bath solution strongly affects the orientation of the physio-chemical properties. The annealed ZnO films synthesized with different contents of H_2O_2 are characterized for their structural, surface morphological, electrical and optical properties.

2. Experimental details

An aqueous solution of 0.1 M $Zn(NO_3)_2$ was prepared, and to this solution aqueous NH_3 solution (28%) was added under constant stirring. A white precipitate was initially observed, which subsequently dissolved upon further addition of NH_3 solution. The H_2O_2 (30 vol.%) was added into the solution with different volumetric proportions, which resulted into decrease in pH of the solution to 11.7. The

* Corresponding author. Tel.: +91 0231 2609225.
E-mail address: l.chandrakant@yahoo.com (C.D. Lokhande).

0925-8388/$ – see front matter © 2011 Elsevier B.V. All rights reserved.
doi:10.1016/j.jallcom.2011.04.094

solution was maintained at a pH ~12 by addition of excess NH_3 solution. A precleaned glass substrate was immersed and placed vertically in the solution. The solution maintained at bath temperature of 348 K for 2 h resulted in the direct growth of nanorods onto the glass substrate. The substrates, with the deposited ZnO nanorods, were thoroughly washed with deionized water to eliminate residual salts. These films were annealed at 673 K for 2 h and used for the further characterization.

The ZnO film thickness was measured with weight difference method using sensitive microbalance. Crystallographic study was carried out using Phillips PW-1710, X-ray diffractometer using Cu K_α ($\lambda = 1.54056$ Å) radiation in the 2θ range from 20 to 80°. The surface morphology was visualized using a scanning electron microscope (SEM). For this, the film was coated with platinum using polaron SEM sputter coating with E-2500. The SEM micrographs were obtained with model JSM-6160. In order to study the fundamental absorption edge, the room temperature optical absorption spectra were recorded in the wavelength range 300–850 nm using UV–vis–NIR spectrophotometer Systronics-119 with glass substrate as a reference. The dark d. c. electrical resistivity of the films was measured using a two-point probe method in the temperature range 300–500 K. Silver paste contacts were used to form electric contacts whose ohmic nature was tested within ±10 V.

3. Results and discussion

3.1. ZnO growth process and reaction mechanism

In chemical method, the small degree of supersaturation causes the heterogeneous nucleation of the metal oxide on the substrates [12]. For Zn^{2+} aqueous solution, the necessary condition for the formation of precipitation is the establishment of ion product higher than solubility product of $Zn(OH)_2$. The degree of supersaturation (S) is the important factor in the examination of the precipitation process in aqueous solution, for the deposition of high quality film from aqueous solution is to control the value of S, to induce the heterogeneous precipitation on the substrates, and to suppress the homogeneous precipitation in the bulk solution. The supersaturation can be controlled by optimizing the preparative parameters such as bath temperature, pH and concentration of resultant solution, to get nanocrystalline thin films.

For the deposition of vertically aligned ZnO nanorods, the mechanism of ZnO film formation can be elucidated as follows: $Zn(NO_3)_2$ was used as a source of Zn^{2+} ions. When ammonia was added to it, white precipitate of $Zn(OH)_2$ was occurred, further addition of ammonia resulted in to dissolution of $Zn(OH)_2$ in to the solution and formation of zincate ($[Zn(NH_3)_4]^{2+}$). The thermal decomposition of $[Zn(NH_3)_4]^{2+}$ releases ions of Zn^{2+} ions reacts with OH^- in the solution and results in the formation of $Zn(OH)_2$ or ZnO particles. Eqs. (1)–(3) illustrate the chemical reaction related to this process [13]:

$$Zn(NO_3)_2 + 2NH_4OH \rightarrow Zn(OH)_2 + 2NH_4NO_3 \quad (1)$$

$$Zn(OH)_2 + 4NH_4OH \rightarrow [Zn(NH_3)_4]^{2+} + 4H_2O + 2OH^- \quad (2)$$

The dilute H_2O_2 added in the bath solution converts $[Zn(NH_3)_4]^{2+}$ into ZnO with the release of oxygen gas in the bath solution at higher temperature. This can be presented by the following reaction:

$$[Zn(NH_3)_4]^{2+} + 2OH^- + H_2O_2 \rightarrow ZnO\downarrow + H_2O + 4NH_3\uparrow + \frac{1}{2}O_2\uparrow \quad (3)$$

The evolution of oxygen gas was practically observed in the form of bubbles during the deposition.

3.1.1. Possible growth mechanism of vertically aligned ZnO nanorods

The vertically aligned ZnO nanorods can be synthesized and possible growth mechanism can be proposed by studying crystal structure of ZnO. With regard to the crystal habits, A typical wurtzite ZnO crystal has polar faces [(0 0 2) plane] and non-polar faces [(1 0 0) and (1 0 1) planes] as shown in Fig. 1(a). Polar faces

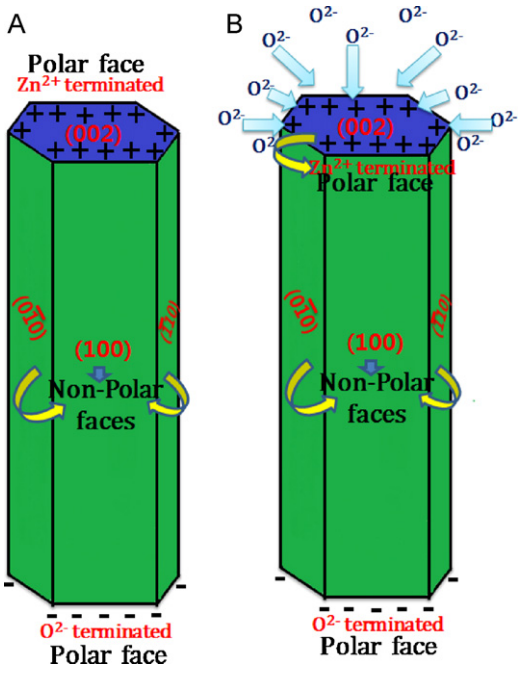

Fig. 1. (a) Crystal structure of ZnO nanorod and (b) growth of nanorods via H_2O_2 route.

with surface dipoles are thermodynamically less stable than non-polar faces which tend to rearrange themselves to minimize surface energy [13]. As a result, the growth along the (0 0 2) plane has faster growth rate than that along other directions. This polarity causes the (0 0 2) face of the crystal either positively or negatively charged. In either case, surface will attract ions of opposite charges (O^{2-} or Zn^{2+}) to it, and this new surface covered with ions will in turn attract ions with opposite charges to cover the surface next and thereby reacting to form ZnO nanorods [14].

In the chemical deposition, the Zn^{2+} and/or O^{2-} ions in the solution are controlled by deposition parameters (bath temperature and pH of the solution) in such a way to form ZnO nanorods. Though the chemical method results into preferential growth along (0 0 2) directions, the growth along other crystallographic planes cannot be avoided. This may result into nanorods but they are tilted. The H_2O_2 is an oxidizing agent used as the source of O^{2-} ions. The additional source of O^{2-} ions promotes the growth of the crystallites along polar (0 0 2) plane [Fig. 1(b)]. The vertically alignment of ZnO nanorods can be achieved by tuning the content of H_2O_2 in the bath solution.

3.2. Thickness measurement

The film thickness was determined gravimetrically by measuring the change in the weight of the substrate due to film deposition and the area with the known density of ZnO ($\rho = 5.675$ g/cm^3) [15]. Fig. 2 shows the variation of thickness of ZnO thin film (with and without H_2O_2) annealed at 673 K with deposition time, plots indicating the usually observed behavior grown by CBD. The growth rate is found to be increased with increasing H_2O_2 content in the bath solution. This may be due to the additional O^{2-} ions provided by the source of oxidizing agent i.e. H_2O_2. ZnO thin films deposited with 2 vol.% of H_2O_2 in the bath solution showed maximum film thickness of 1.86 μm (for the deposition time of 120 min). The ZnO thin films deposited for 100 min from the bath containing 0, 1 and 2 vol.% of H_2O_2 in the bath solution and annealed at 673 K are hereafter referred as samples ZH1, ZH2 and ZH3, respectively.

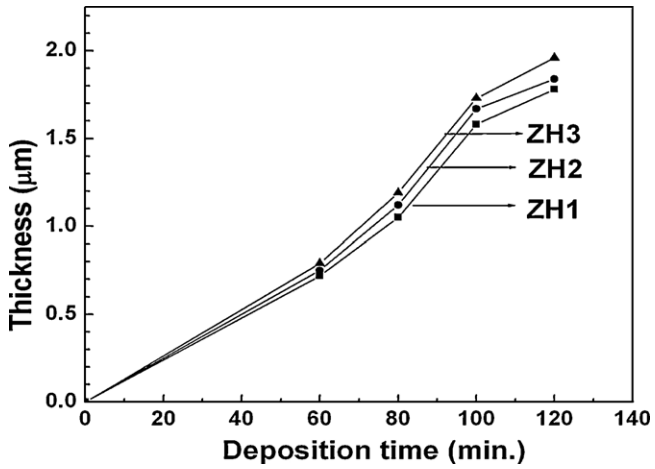

Fig. 2. Variation of film thickness with deposition time for samples ZH1, ZH2 and ZH3.

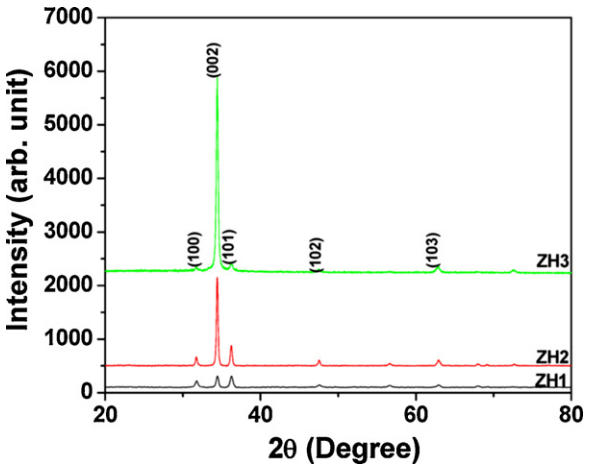

Fig. 3. X-ray diffractograms of (a) ZH1 (b) ZH2 and (c) ZH3 samples.

3.3. X-ray diffraction studies

Fig. 3(a)–(c) shows the XRD patterns of the ZnO films deposited with different contents of H_2O_2 in the bath solution. All diffraction peaks can be indexed as ZnO crystal with hexagonal wurtzite structure (JCPDS card no. 36-1451). It is interesting to note that from figure, with increasing the content of H_2O_2, diffraction intensity of the peak, assigned to (0 0 2) plane, is markedly increased and that from the other crystal planes are found to be decreased. This implies that, the crystallites are oriented strongly along *c*-axis. This may be due to the inhabitant growth of ZnO crystal along *c*-axis, which is further promoted by adding H_2O_2 in the bath solution, which acts as the source of O^{2-} ions. The oriented growth by adding H_2O_2 in the solution has been observed for PbS crystal [16]. Table 1 gives the comparison of standard and observed '*d*' values and intensities for ZnO films deposited with different H_2O_2 content (sample ZH1–ZH3).

It is striking that, the orientation of ZnO nanorods can be controlled by content of H_2O_2 in the bath solution which reflects in terms of the texture coefficient $R_{\text{texture}\,(hkl)}$. Fig. 4 shows the variation of texture coefficient R_{texture} for (0 0 2) plane with vol.% of H_2O_2 in the bath solution. Maximum texture coefficient R_{texture} for (0 0 2) plane obtained for sample ZH3 shows that the degree of alignment of ZnO nanorods is 89%. The alignment is as good as those obtained in earlier studies of ZnO nanorods grown by low temperature solution method [17], wherein the substrates used were preseeded with ZnO nanoparticles in order to provide nucleation sites.

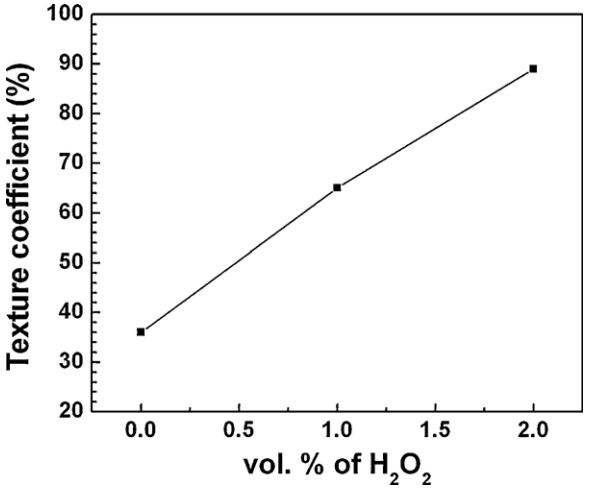

Fig. 4. Variation of texture coefficient with content of H_2O_2 in the bath solution.

3.4. Surface morphological studies

Fig. 5(a)–(f) shows the SEM micrographs, with two different magnifications, of ZnO thin films deposited with different contents of H_2O_2. Fairly, well defined hexagonal facets, entangled nanorods; typically having diameter 150 nm observed for sample ZH1. Such nanorods are arranged in a very large, uniform array, which covers entire surface of the glass substrate, as can be seen from Fig. 5(a). Well defined crystallographic faces i.e. polar terminated (0 0 2) and non-polar (1 0 1) faces can clearly be identified [Fig. 5(b)]. Addition of H_2O_2 (1 vol.%) causes crystal to orient perpendicular to the substrate surface, as shown in Fig. 5(c) and (d). With more H_2O_2 (2 vol.%), vertically aligned ZnO nanorods are observed as shown in Fig. 5(e) and (f). This is attributed to increased orientation of ZnO nanorods by increasing H_2O_2 content in the bath solution. Fig. 5(g) shows the cross sectional view of the vertically aligned ZnO nanorods deposited with 2 vol.% of H_2O_2. It is seen that the ZnO crystals grow along *c*-axis and form vertically aligned ZnO nanorods.

Table 1
Comparison between standard and observed '*d*' values and intensities of samples ZH1, ZH2 and ZH3.

Sr. no	Std '*d*' (Å)	Sample ZH1		Sample ZH2		Sample ZH3		(*h k l*)
		d (Å)	*I* (a. u.)	*d* (Å)	*I* (a. u.)	*d* (Å)	*I* (a. u.)	
1	2.81	2.81	127	2.81	102	2.81	122	1 0 0
2	2.60	2.60	221	2.60	1600	2.60	3672	0 0 2
3	2.47	2.47	217	2.47	222	2.47	185	1 0 1
4	1.91	1.91	48	1.91	86	–	–	1 0 2
5	1.62	1.62	39	1.62	25	–	–	1 1 0
6	1.47	1.47	52	1.47	142	1.47	165	1 0 3
7	1.37	1.37	23	–	–	–	–	1 1 2

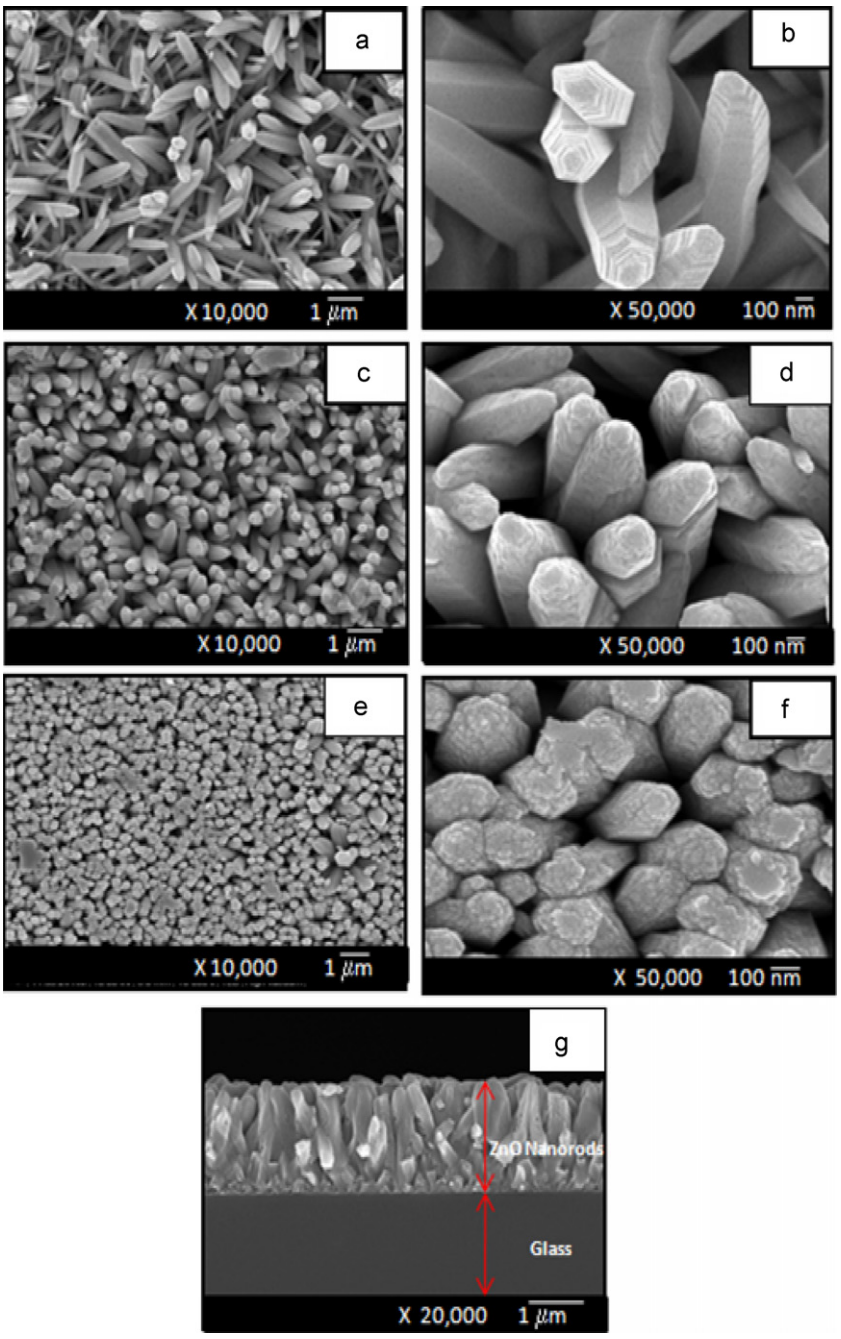

Fig. 5. (a–f) Scanning electron micrographs of sample ZH1, ZH2 and ZH3 at two different magnifications (10,000× and 50,000×) and (g) cross-sectional view of the sample ZH3.

Fig. 6 represents relative position of (1 0 0), (1 0 1), (1 0 3) and (0 0 2) planes in the ZnO lattice. As can be seen from Fig. 6, the inclination angles between (0 0 2) and (1 0 3), (0 0 2) and (1 0 1), and (0 0 2) and (1 0 0) are 31.6°, 61.6° and 90.0°, respectively. As the H_2O_2 content increased, the crystals formed in the films are gradually oriented, which led to the (0 0 2) planes lying perpendicular to the substrate surface in sequence [18].

3.5. Electrical resistivity measurements

The dark d. c. electrical resistivity measurement of films was carried out using two-point probe method within temperature range of 300–500 K. Fig. 7 shows the variation of $\log \rho$ against $1000/T$ for samples ZH1, ZH2 and ZH3. It is observed for all the samples that, resistivity of the sample decreases with increasing temperature, indicating the semiconducting nature of the samples. The room temperature electrical resistivity of sample ZH1 is $1.99 \times 10^3\ \Omega$ cm, which is decreased to $1.58 \times 10^3\ \Omega$ cm for sample ZH2 and to $1.02 \times 10^3\ \Omega$ cm for sample ZH3. The decrease in room temperature resistivity with increase in orientation of the nanorods may be due to the fact that the oriented nanorods provides direct path for efficient electron transfer than the entangled nanorods [19].

3.6. Optical properties

The UV–vis absorption spectra of samples ZH1, ZH2 and ZH3 were studied at room temperature without taking into account the

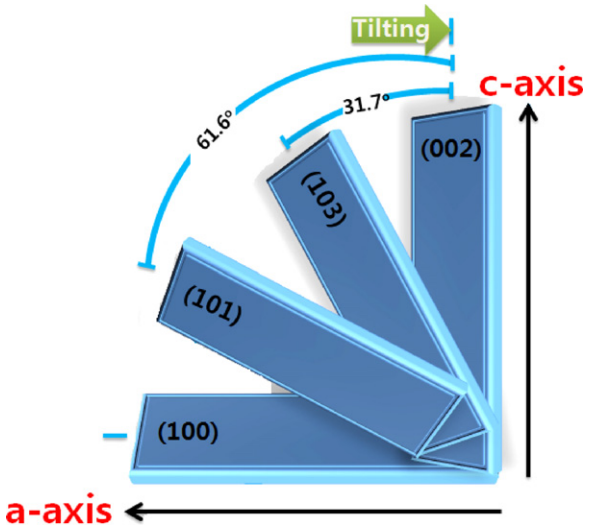

Fig. 6. Schematic illustration shows the relative position of (1 0 0), (1 0 1), (1 0 3), and (0 0 2) planes in the ZnO lattice.

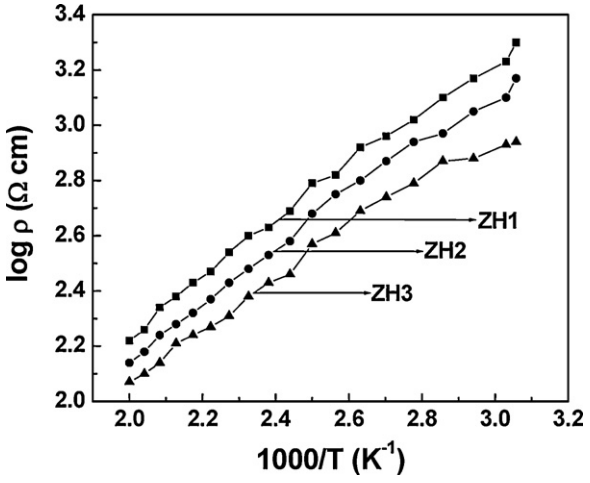

Fig. 7. Variation of electrical resistivity of ZnO films with reciprocal of temperature (1000/T) of samples ZH1, ZH2, and ZH3.

reflection and transmission losses. The absorption spectra [Fig. 8(a)] reveal that, all the samples have low absorbance in the visible region of the solar spectrum. However, with increased content of H_2O_2, the absorbance is increased with 'blue shift' in the absorption edge. The increased absorbance with increased content of H_2O_2 in the bath solution can be attributed to the increase in the film thickness, as mentioned in Section 3.2. The similar type of solvent effect on the optical properties of ZnO thin films has been studied by Wang et al. [18]. From, Fig. 8(b) the bandgap is found to be increased from 3.20 to 3.38 eV with increased content of H_2O_2 in the bath solution. The 'E_g' values are in good agreement with value reported for ZnO nanorods [20].

4. Conclusions

In conclusion, the vertically aligned arrays of ZnO nanorods are grown onto glass substrate by CBD method via H_2O_2 route. The possible growth mechanism for the vertically aligned ZnO nanorods is proposed. Content of H_2O_2 in the bath solution strongly affected the structural, morphological, electrical and optical properties. Crystallites are strongly oriented along (0 0 2) plane with increased H_2O_2 content in the bath solution showing textured growth along

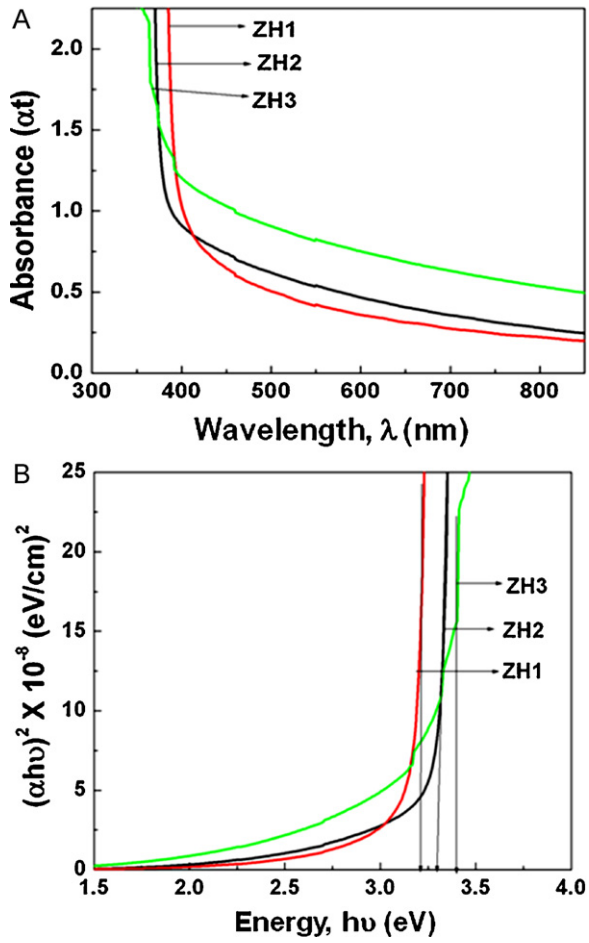

Fig. 8. (a) The variation of absorbance (αt) with wavelength (λ) of samples ZH1, ZH2 and ZH3 and (b) plots of $(\alpha h\upsilon)^2$ versus $h\upsilon$ of samples ZH1, ZH2 and ZH3.

c-axis. Morphological study revealed entangled nanorods oriented vertically along c-axis with increased H_2O_2 content in the bath solution. The decrease in room temperature resistivity is observed with increase in content of H_2O_2 in the bath solution. The optical direct bandgap is found to increase from 3.2 to 3.4 eV, as the content of H_2O_2 in the bath solution is increased.

Acknowledgement

Authors are grateful to the Department of Science and Technology, New Delhi for financial support through the scheme no. SR/S2/CMP-82/2006.

References

[1] H. Bahadur, A.K. Shrivastava, R.K. Sharma, S. Chanda, Nanoscale Res. Lett. 2 (2007) 469.
[2] M. Huang, Y. Wu, S. Mao, H. Fick, H. Yan, H. Kind, E. Webber, R. Russo, P. Yang, Science 292 (2001) 1897.
[3] M. Huang, Y. Wu, H. Fick, N. Tran, E. Webber, P. Yang, Adv. Mater. 13 (2001) 113.
[4] J.Y. Park, H. Oh, J.J. Kim, S.S. Kim, J. Cryst. Growth 287 (2006) 145.
[5] T. Okada, B.H. Agung, Y. Nakata, Appl. Phys. A 79 (2004) 1417.
[6] R. Liu, A.A. Vertegel, E.W. Bohannan, T.A. Sorenson, J.A. Switzer, Chem. Mater. 13 (2001) 508.
[7] L. Vayssieres, Adv. Mater. 15 (2003) 464.
[8] H. Sun, M. Luo, W. Weng, K. Cheng, P. Du, G. Shen, G. Han, Nanotechnology 19 (1) (2008) 25603.
[9] A. Ennaoui, M. Weber, R. Scheer, H.J. Lewerenz, Sol. Energy Mater. Sol. Cells 54 (1998) 277.
[10] K.V. Gurav, V.J. Fulari, U.M. Patil, C.D. Lokhande, O.S. Joo, Appl. Surf. Sci. 256 (2010) 2680.
[11] S. Peulon, D. Lincot, Adv. Mater. 8 (1996) 166.

[12] B.C. Bunker, P.C. Rieeke, B.J. Tarasevich, A.A. Campbell, G.E. Fryxell, G.L. Graff, L. Song, J. Liu, W. Virden, G.L. McVay, Science 264 (1994) 48.
[13] P.K. Samanta, S.K. Patra, P. Roy Chaudhuri, Physica E 11 (2008) 1.
[14] Q. Li, V. Kumar, Y. Li, H. Zhang, T.J. Marks, R.P.H. Chang, Chem. Mater. 17 (2005) 1001.
[15] D.R. Lind (Ed.), CRC Handbook of Physics and Chemistry, 79th edition, New York, 1998–1999.
[16] L.C. Torriani, M. Tomyiama, S. Bilac, G.B. Rego, J.I. Cisneros, Z.P. Argüello, Thin Solid Films 77 (1981) 347.
[17] R. Chander, A.K. Raychaudhuri, J. Mater. Sci. 41 (2006) 3623.
[18] M. Wang, S.H. Han, E.J. Kim, J.S. Kim, S. Kim, C. Park, K.K. Koo, Thin Solid Films 516 (2008) 8599.
[19] J.X. Wang, X.W. Sun, Y. Yang, H. Huang, Y.C. Lee, O.K. Tan, L. Vayssieres, Nanotechnology 17 (2008) 4995.
[20] H. Xue, X.L. Xu, Y. Chen, G.H. Zhang, S.Y. Ma, Appl. Surf. Sci. 255 (2008) 1806.